2

Imaging at the atomic scale

Scanning Tunneling Microscopy (STM)

Atomic Force Microscopy (AFM)

Exercise 2.1

Scanning Probe Microscopy

Introduction to Scanning Tunneling Microscopy
C. J. Chen
Oxford University Press

Scanning Probe Microscopy and Spectroscopy
R. Wiesendanger
Cambridge University Press

Scanning Probe Microscopy
B. Voigtländer
Springer

Surface science techniques, UHV

Physics of Surfaces and Interfaces
H. Ibach
Springer

Surface Science - An Introduction
K.Oura, V. G. Lifshits, A. A. Saranin, A.V. Zotov, M. Katayama
Springer

Scanning Tunneling Microscope (STM)

Idea

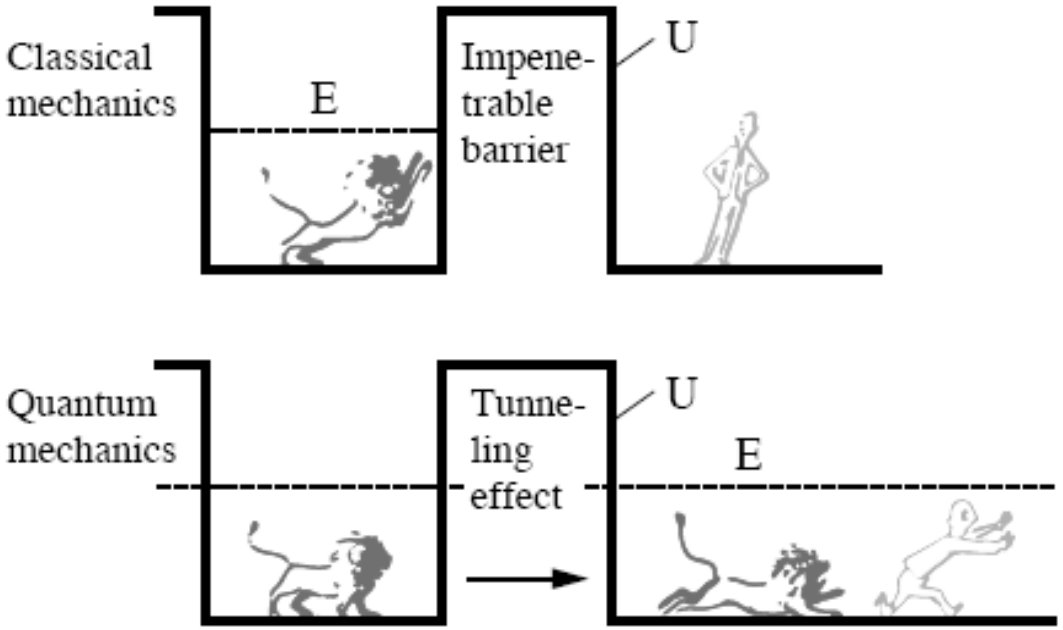

The difference between classical theory and quantum theory. In quantum mechanics, an electron has a nonzero probability of tunneling through a potential barrier. (After Van Vleck; see Walmsley, 1987.)

Working principle

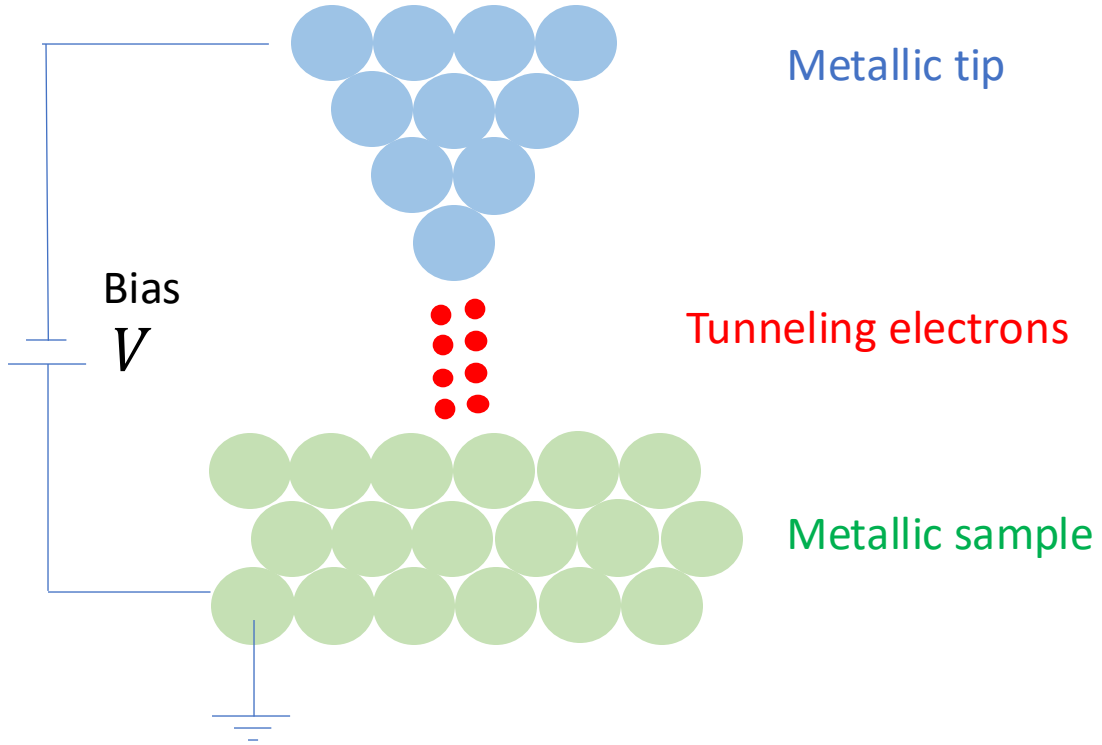

One-dimensional potential barrier model

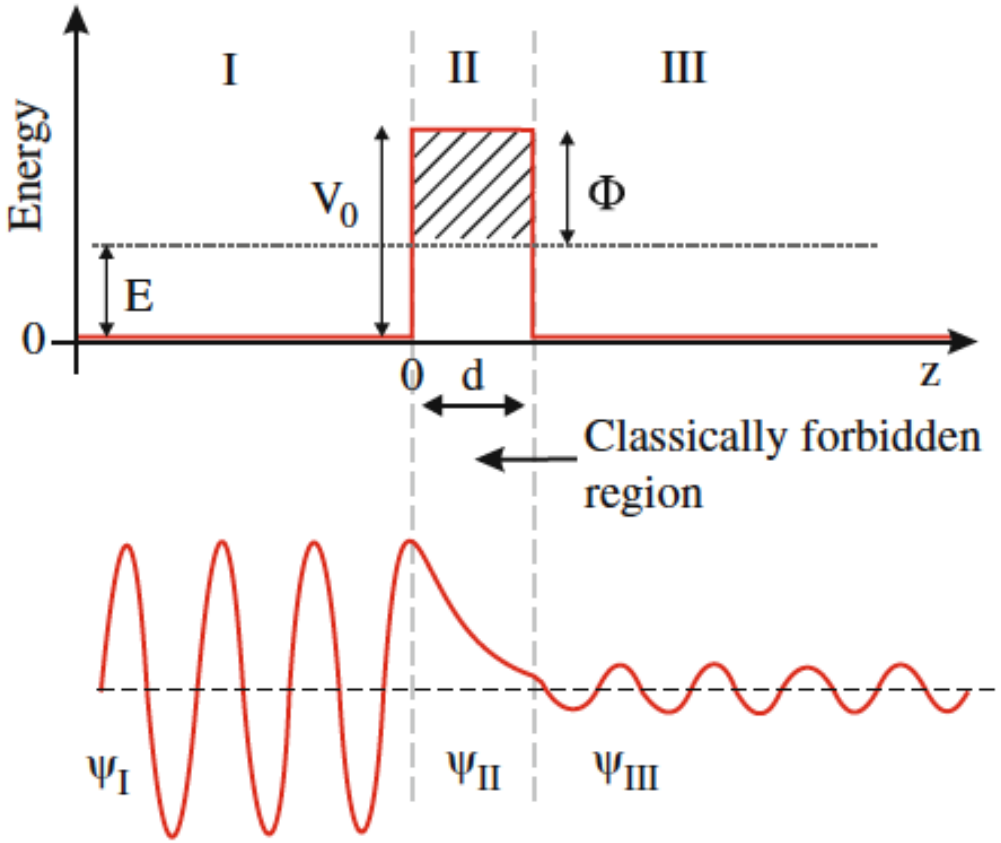

$$\psi(z) = \psi(0)e^{-\kappa z}$$

in region II (classically forbidden), exponential decay:

$$\psi(z) = \psi(0)e^{-\kappa z}$$

with $$\kappa = \frac{\sqrt{2m(V_0 - E)}}{\hbar}$$

in particular $$\psi(d) = \psi(0)e^{-\kappa d}$$

→ tunneling probability and current

$$\propto |\psi(d)|^2 = |\psi(0)|^2 e^{-2\kappa d}$$

Bardeen model for tunneling

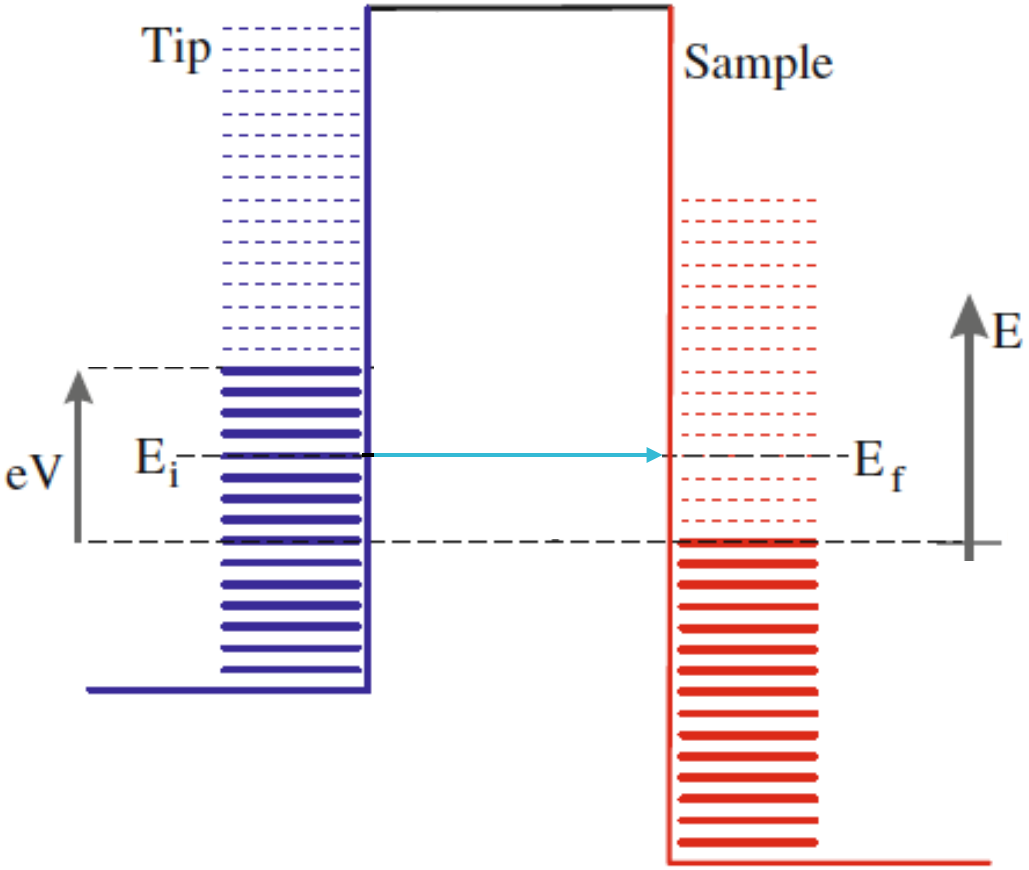

We apply for example a positive bias to the sample, shifting the energy levels of tip and sample.

Perturbative approach: start with eigenfunctions and respective energy levels.

initial state final state

$\psi_{\mathrm{tip},i}$ E_i $\psi_{\mathrm{sample},f}$ E_f

The transition probability per unit time $w_{i\to f}$ of an electron from the tip state $\psi_{\mathrm{t},i}$ to the sample state $\psi_{\mathrm{s},f}$ is given by the Fermi golden rule (energy conservation, elastic tunneling):

$$w_{i\to f} = \frac{2\pi}{\hbar}\left|M_{fi}\right|^2 \delta\left(E_f - E_i\right)$$

The tunneling matrix element is determined by a surface integral on a surface between the two electrodes, giving the current density probability (continuity equation):

$$M_{fi} = \frac{\hbar^2}{2m}\iint\left(\psi_{\mathrm{t},i}\,\boldsymbol{\nabla}\psi^*_{\mathrm{s},f} - \psi^*_{\mathrm{s},f}\,\boldsymbol{\nabla}\psi_{\mathrm{t},i}\right)\cdot d\boldsymbol{S}$$

DOI: 10.1103/PhysRevLett.6.57
J. Bardeen, Phys. Rev. Lett. **6**, 57 (1961).

Bardeen model for tunneling

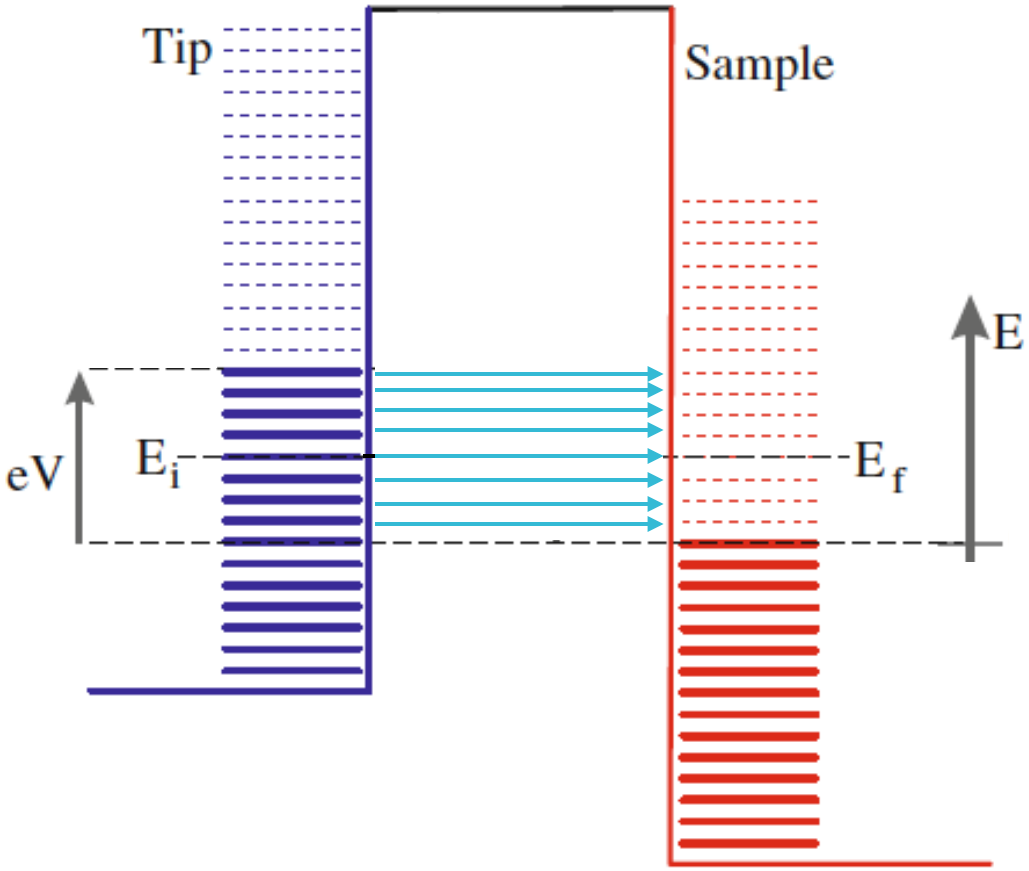

Total rate: sum over all pairs of initial and final states

$$w_{\text{tip}\to\text{sample}} = \frac{2\pi}{\hbar}\sum_{i,f}\left|M_{fi}\right|^2 \delta\left(E_f - E_i\right)$$

To get the current, we multiply the transition rate by the electron charge.
Considering the spin and neglecting the sign of the charge:

$$I_{\text{tip}\to\text{sample}} = \frac{4\pi e}{\hbar}\sum_{i,f}\left|M_{fi}\right|^2 \delta\left(E_f - E_i\right)$$

Bardeen model for tunneling

Exercise 2.2

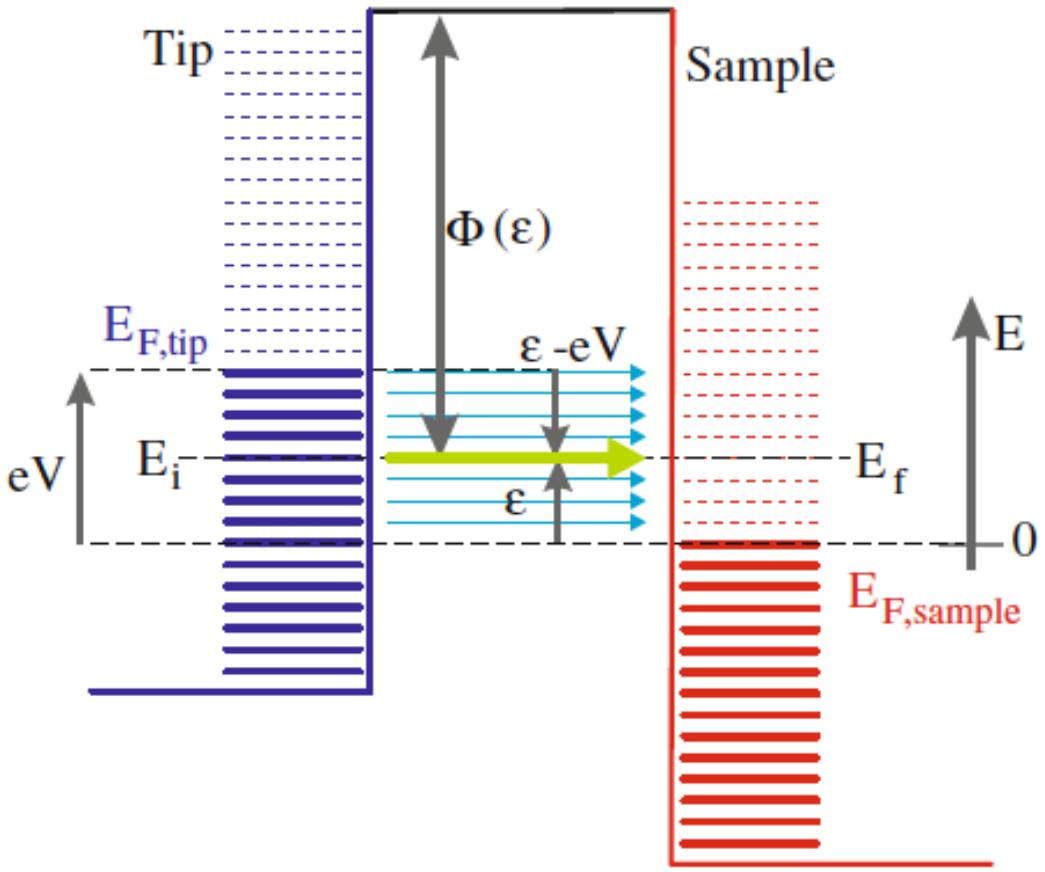

The tunneling current is a convolution of states of sample and tip

discrete levels → density of states

number of states with energy between E and $E + dE$:

$$dN(E, E + dE) = \rho(E)dE \qquad \rho(E) = \sum_n \delta(E - E_n)$$

$$M_{fi} = M(E_f, E_i) = M(E_i)$$

Using the properties of the Dirac delta function δ and the definition of ρ :

$$I_{\text{tip}\to\text{sample}} = \frac{4\pi e}{\hbar} \int_{E_{F,\text{sample}}}^{E_{F,\text{tip}}} \rho_t(\varepsilon)\rho_s(\varepsilon)\,|M(\varepsilon)|^2 d\varepsilon$$

Using $E_{F,\,\text{sample}} = 0$ as reference and expressing the energy of each electrode with respect to "its own" Fermi level:

$$I_{\text{tip}\to\text{sample}} = \frac{4\pi e}{\hbar} \int_0^{eV} \rho_t(\varepsilon - eV)\rho_s(\varepsilon)\,|M(\varepsilon)|^2 d\varepsilon$$

Bardeen model for with 1D rectangular barrier

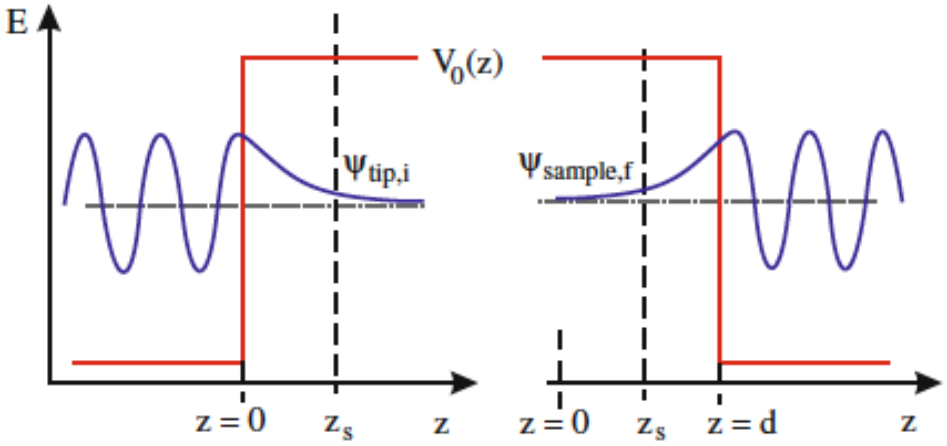

Evaluation of the tunneling matrix element $M(E)$ is difficult (3D barrier)

Simplification: 1D rectangular barrier

$$M(E) = \frac{\hbar^2}{2m} \int_{z=z_{surf}} \left[\psi_{tip}(z,E) \frac{\partial \psi^*_{sample}(z,E)}{\partial z} - \partial \psi^*_{sample}(z,E) \frac{\partial \psi_{tip}(z,E)}{\partial z} \right] dS$$

$$\psi_{tip}(z) = \psi_{tip}(0) e^{-\kappa z}$$

$$\psi_{sample}(z) = \psi_{sample}(d) e^{-\kappa(d-z)}$$

$$M(E) = \frac{\hbar^2}{2m} \int_{z=z_{surf}} 2\,\kappa\,\psi_t(0)\,\psi_s(d)\,e^{-\kappa z_{surf}}\,e^{\kappa(z_{surf}-d)} dS \quad \propto \quad \frac{\hbar^2}{m}\kappa\;\psi_t(0)\,\psi_s(d)\;e^{-\kappa d}$$

The energy dependence is dominated by the contribution of κ in the exponential term

1D: transmission factor $\quad |M(E)|^2 = T(\Phi, d) \propto \exp(-2\kappa d) = \exp\left(-2d\sqrt{\frac{2m}{\hbar^2}\Phi}\right)$ $\qquad \Phi = V_0 - E$

Average barrier height

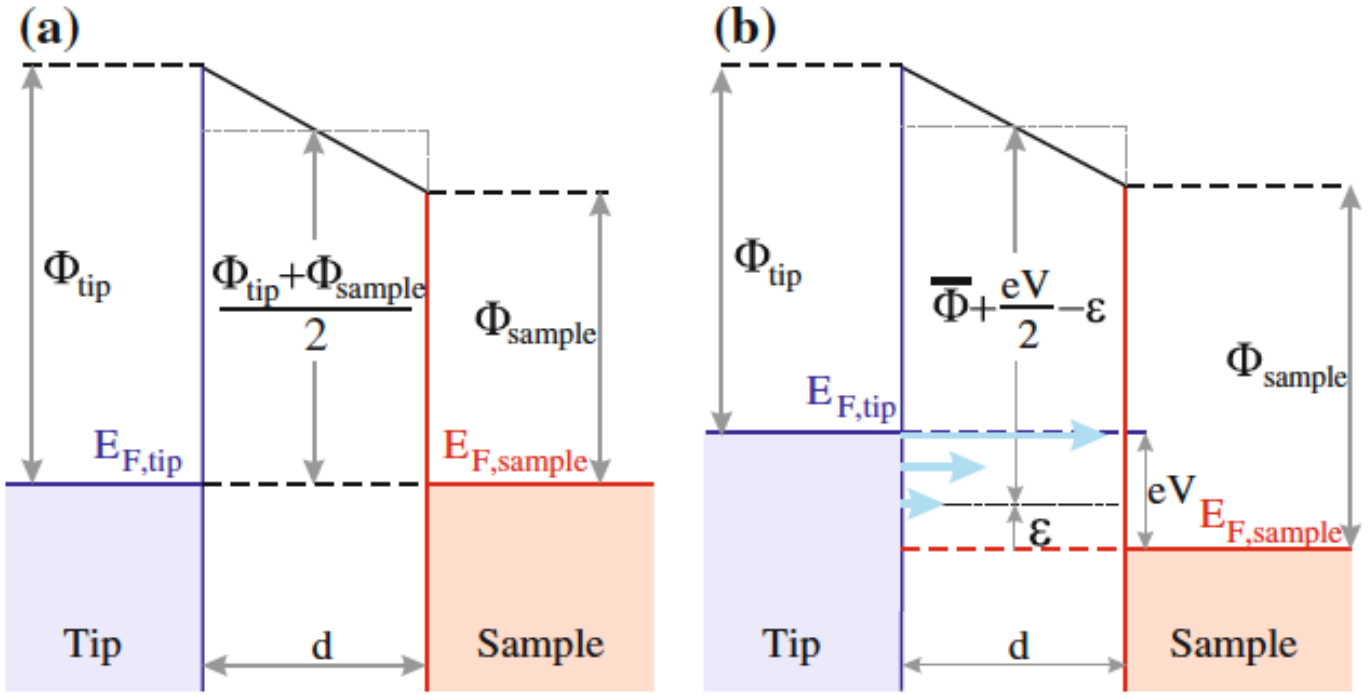

what to put as realistic Φ

$$T(\varepsilon, \Phi, d) \propto \exp\left(-2d\sqrt{\frac{2m}{\hbar^2}\left(\frac{\Phi_{\text{tip}}+\Phi_{\text{sample}}}{2}+\frac{eV}{2}-\varepsilon\right)}\right)$$

Tunneling current – Small bias limit

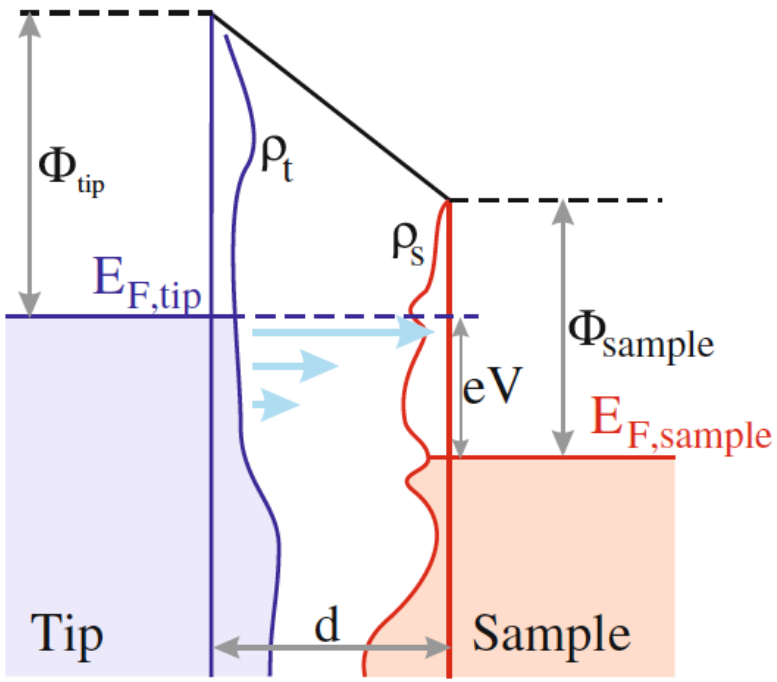

Current in Bardeen model for a one-dimensional barrier in the limit of zero temperature:

$$I = \frac{4\pi e}{\hbar} \int_0^{eV} \rho_t(\varepsilon - eV)\rho_s(\varepsilon)\, T(\varepsilon, V, d)\, d\varepsilon$$

For small bias $(eV \ll \Phi)$

- transmission factor independent of bias and energy

$$I = \frac{4\pi e}{\hbar}\, T(d) \int_0^{eV} \rho_t(\varepsilon - eV)\rho_s(\varepsilon)\, d\varepsilon$$

- density of states can be considered as constant, equal to the density of states at E_F

$$I \propto \rho_t(E_F)\, \rho_s(E_F)\, V\ \exp(-2\kappa d)$$

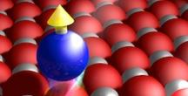

Tunneling current - Small bias limit

$$I \propto V \rho_t(E_F)\, \rho_s(E_F)\, \exp(-2\kappa d)$$

$$\kappa = \frac{\sqrt{2m\,\bar{\Phi}}}{\hbar}$$

$\bar{\Phi}$ average of Φ_t and Φ_s

typical work function of metals is 4-5 eV

with Φ= 4 eV → $\kappa = \frac{\sqrt{2m\,\Phi}}{\hbar} = 0.51\sqrt{\Phi(\mathrm{eV})}$ Å^{-1} ~ 1 Å^{-1}

variation of distance d by Δz:

Δz =1 Å → $\exp(-2\kappa\,\Delta z) \sim \exp(-2) \sim 0.13$

$$I \propto V \rho_t(E_F) \rho_s(E_F) e^{-1.025\sqrt{\Phi}\, d}$$

Φ in [eV]; d in [Å]

For electrons at the Fermi level E_F of sample or tip, a variation in distance of 1 Å results in one order of magnitude difference in the tunneling probability

Tunneling current – Finite temperature

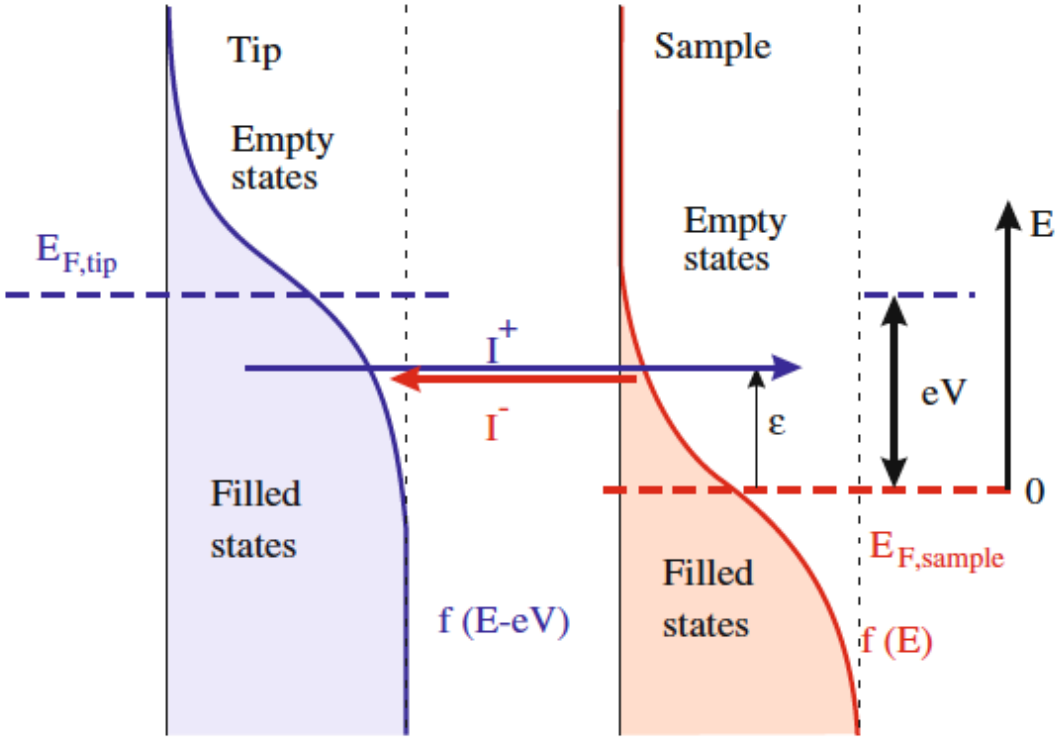

$$I^+(E) = I_{\mathrm{t,\,filled\rightarrow s,empty}} \propto f\left(E - E_{F,\mathrm{t}}\right) \cdot \left[1 - f\left(E - E_{F,\mathrm{s}}\right)\right]$$

$$I^-(E) = I_{\mathrm{s,\,filled\rightarrow t,empty}} \propto f\left(E - E_{F,\mathrm{s}}\right) \cdot \left[1 - f\left(E - E_{F,\mathrm{t}}\right)\right]$$

$$I(E) = I^+ - I^- \propto f\left(E - E_{F,\mathrm{t}}\right) - f\left(E - E_{F,\mathrm{s}}\right)$$

$$I = \frac{4\pi e}{\hbar} \int_0^{eV} \left[f(\varepsilon - \mathrm{eV}) - f(\varepsilon)\right] \rho_t(\varepsilon - eV)\ \rho_{\mathrm{s}}(\varepsilon)\ T(\varepsilon, V, d)\, d\varepsilon$$

occupation of states described by the Fermi-Dirac function

$$f(E - E_F) = \frac{1}{1+\exp[(E-E_F)/k_B T]}$$

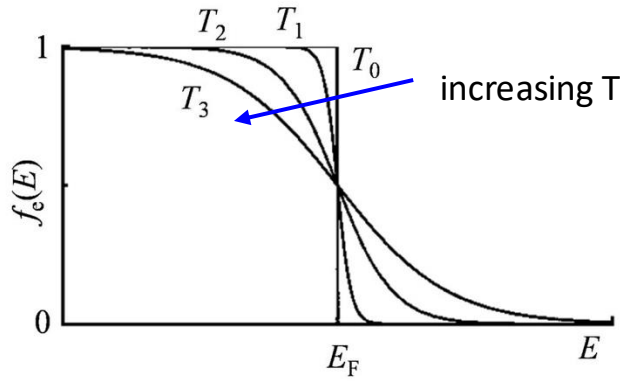

Bias polarity

All treatment so far

Positive bias, tunneling from tip occupied states to sample empty states

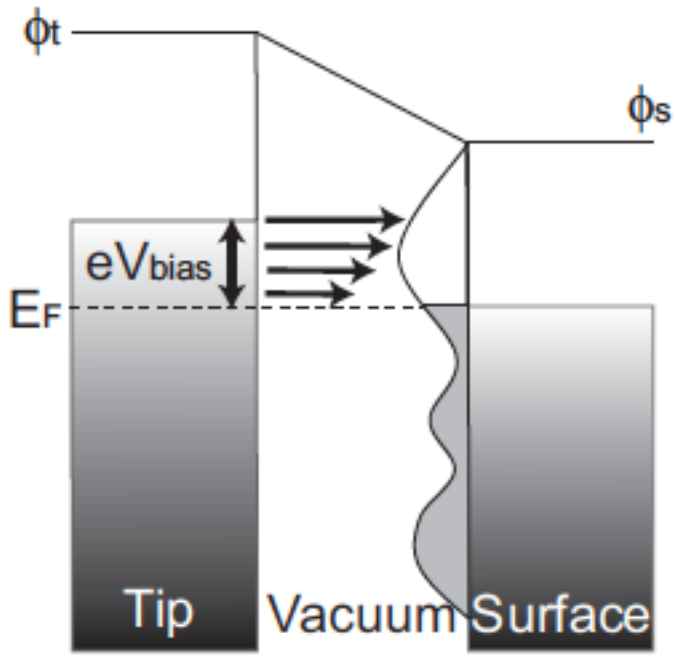

Changing bias polarity → change in the direction of the tunneling current

Negative bias, tunneling from sample occupied states to tip empty states

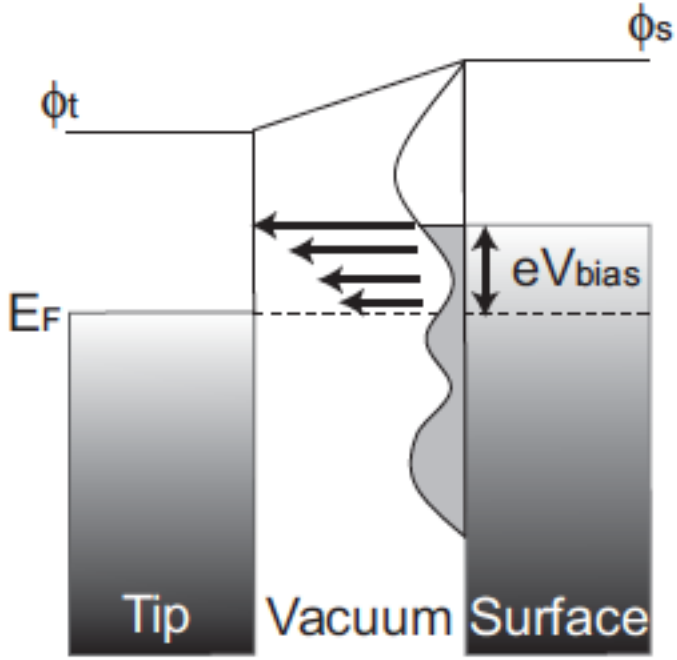

Exercises 2.3 – 2.4

$$I \propto V\rho_t(E_F)\rho_s(E_F)e^{-1.025\sqrt{\Phi}d}$$

Φ in [eV]; d in [Å]

Typical Φ = 4 - 5 eV

Set point (although not really very low bias): $V = 1\ \text{V};\ I = 1\ \text{nA} \rightarrow d \sim 5\ \text{Å}$

Atomic step: $\Delta d = 2\ \text{Å}$

$d - \Delta d$: $\dfrac{\Delta I}{I} \approx e^{1.025\sqrt{\Phi}\,\Delta d} - 1 \approx 50 \text{ to } 100$

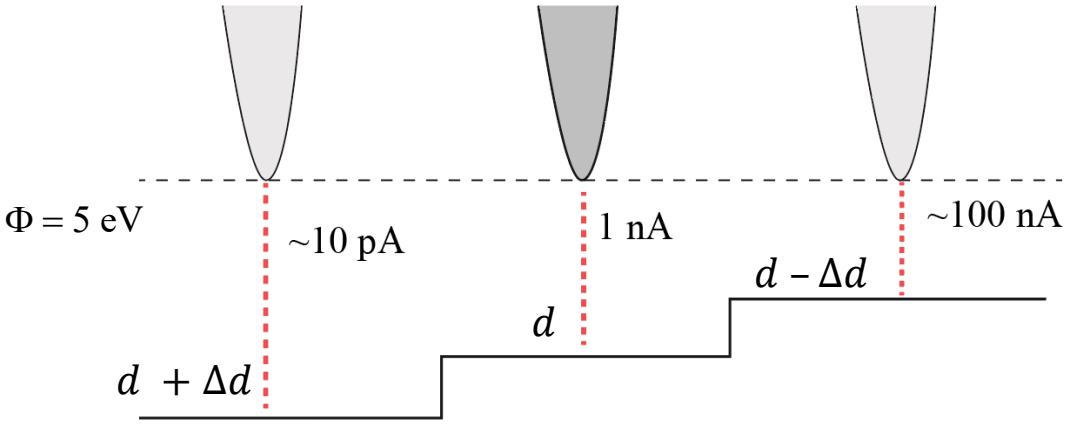

Atomic corrugation: $\Delta d = 0.2\ \text{Å}$

$d - \Delta d$: $\dfrac{\Delta I}{I} \approx e^{1.025\sqrt{\Phi}\,\Delta d} - 1 \approx 0.5$

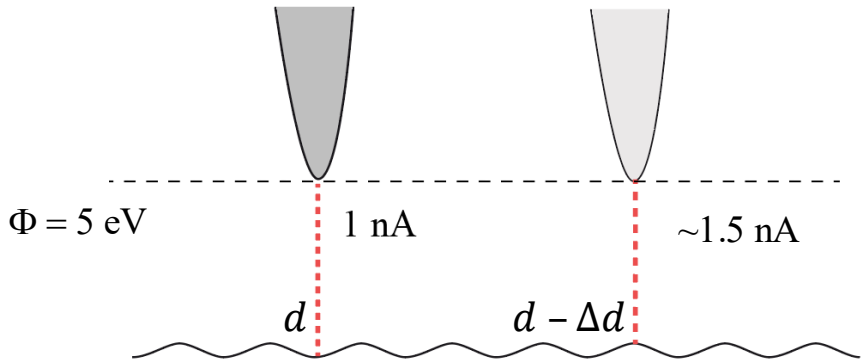

Tersoff-Hamann approximation of the Bardeen model

Different approach to describe the tunneling matrix element M:

Neglect its energy dependence and evaluate M in the **limit of small voltages**, i.e., at the Fermi level

Expressions of wavefunctions are needed
Simplest STM tip: s-orbital wave function

If the position of the tip is $\boldsymbol{r}_0$, the current at small voltages reduces to

$$I \propto \sum_n |\psi_n(\boldsymbol{r}_0)|^2 \, \delta(E_F - E_n) \equiv \rho_{\text{sample}}(E_F, \boldsymbol{r}_0)$$

LDOS: local density of states

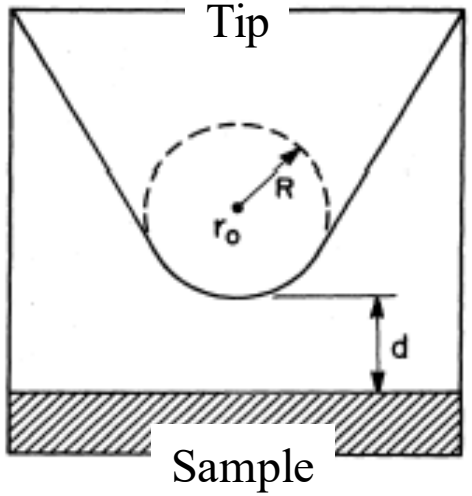

→ the STM measures the LDOS of the surface at the Fermi level at the tip location

DOI: 10.1103/PhysRevB.31.805
J. Tersoff and D. R. Hamann, Phys. Rev. B **31**, 805 (1985)

STM – atomic corrugation

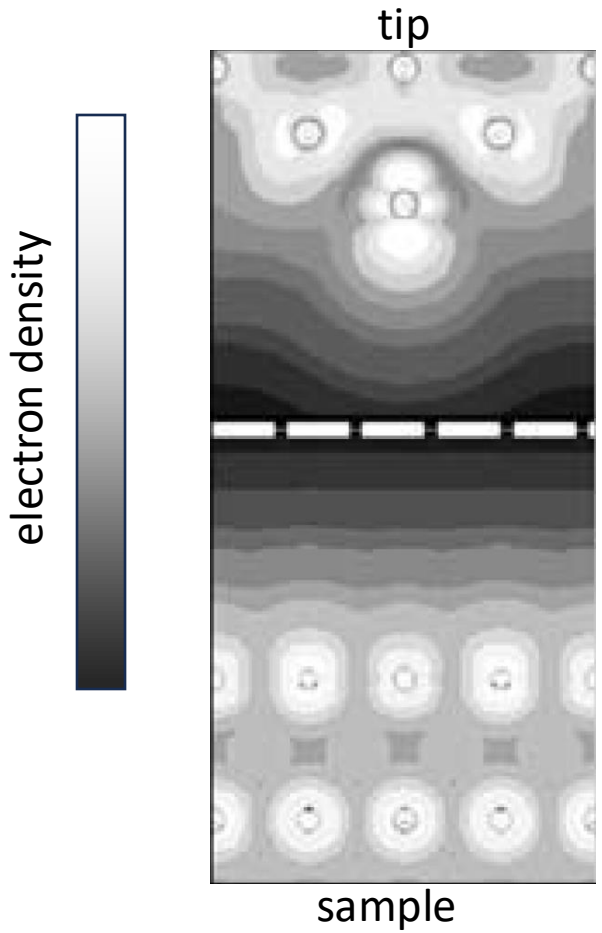

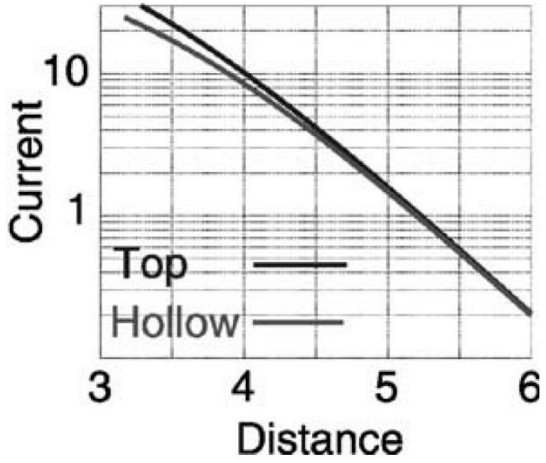

DOI: 10.1016/S0079-6816(03)00005-4
W. A. Hofer, Prog. Surf. Sci. **71**, 147 (2003)

Role of atomic states (orbitals) of tip and sample

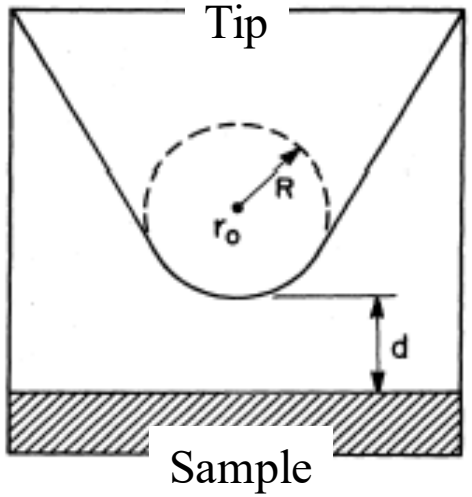

$$I \propto V\rho_s(E_F, r_0)\,\rho_t(E_F)\,e^{-1.025\sqrt{\Phi}d}$$

Orbital shape

s 

p_z 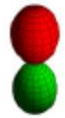

d_{z^2} 

Tersoff-Hamann approximation:
tip density of states ρ_t originating from s-orbitals

but ρ_t can play a role in improving the spatial resolution

Role of atomic states (orbitals) of tip and sample

Exercise 2.5

Corrugation dependence on tip and sample electronic state

Tip state	Sample state	Corrugation amplitude $\Delta z(z)$	Ratio
s	s	$[9\kappa/\gamma^2]\ \exp\{-[\gamma-2\kappa]z\}$	1
s	p	$[\gamma/2\kappa]^2[9\kappa/\gamma^2]\ \exp\{-[\gamma-2\kappa]z\}$	2.73
s	d	$\{(3/2)[(\gamma/2\kappa)^2-(1/3)]\}^2[9\kappa/\gamma^2]\ \exp\{-[\gamma-2\kappa]z\}$	12.9
p	s	$[\gamma/2\kappa]^2[9\kappa/\gamma^2]\ \exp\{-[\gamma-2\kappa]z\}$	2.73
p	p	$[\gamma/2\kappa]^4[9\kappa/\gamma^2]\ \exp\{-[\gamma-2\kappa]z\}$	7.45
p	d	$[\gamma/2\kappa]^2\{(3/2)[(\gamma/2\kappa)^2-(1/3)]\}^2[9\kappa/\gamma^2]\ \exp\{-[\gamma-2\kappa]z\}$	35.2
d	s	$\{(3/2)[(\gamma/2\kappa)^2-(1/3)]\}^2[9\kappa/\gamma^2]\ \exp\{-[\gamma-2\kappa]z\}$	12.9
d	p	$[\gamma/2\kappa]^2\{(3/2)[(\gamma/2\kappa)^2-(1/3)]\}^2[9\kappa/\gamma^2]\ \exp\{-[\gamma-2\kappa]z\}$	35.2
d	d	$\{(3/2)[(\gamma/2\kappa)^2-(1/3)]\}^4[9\kappa/\gamma^2]\ \exp\{-[\gamma-2\kappa]z\}$	166

Orbital shape

s

p_z

dz^2

Materials with highly directional electronic orbitals give better resolution

TABLE I. Fermi-level DOS of common tip materials (Ref. 13).

Material	W	Pt	Ir
s state	3.1%	0.77%	0.94%
d state	85%	98%	96%

DOI: 10.1103/PhysRevB.42.884
C. J. Chen. *Phys. Rev. B*. **42**, 8841 (1990)
DOI: 10.1116/1.577128
C. J. Chen. *J. Vac. Sci. Technol. A* **9**, 44 (1991)

Tip preparation

Tungsten wire

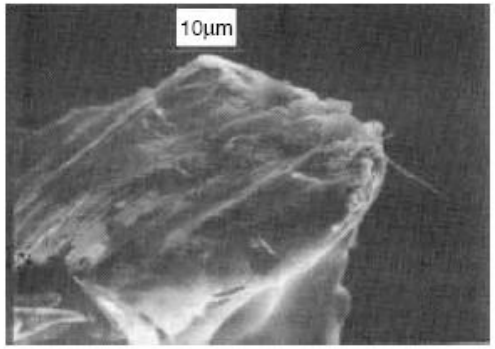

After electro-erosion (etching)

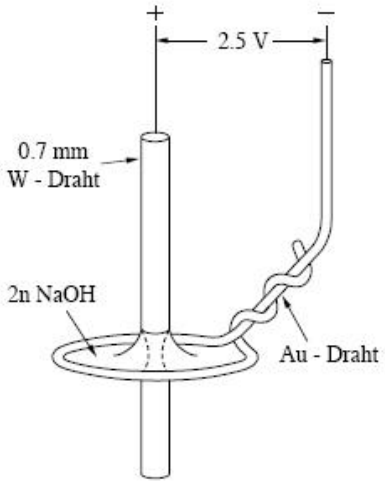

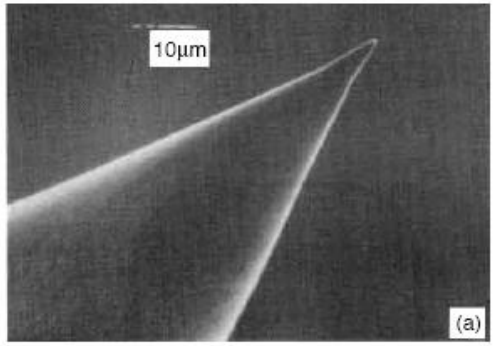

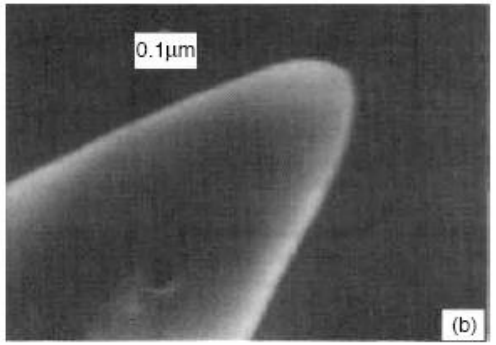

Platinum/Iridium wire

$Pt_{90}Ir_{10}$
$Pt_{80}Ir_{20}$

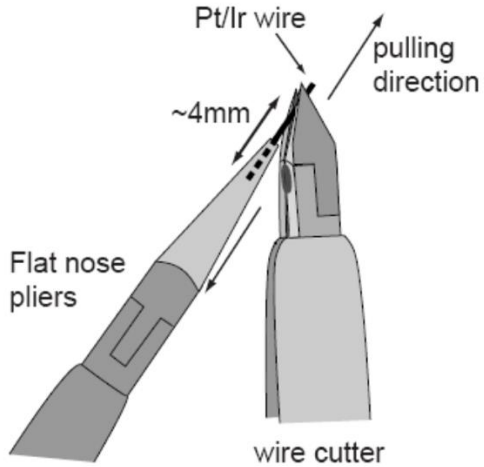

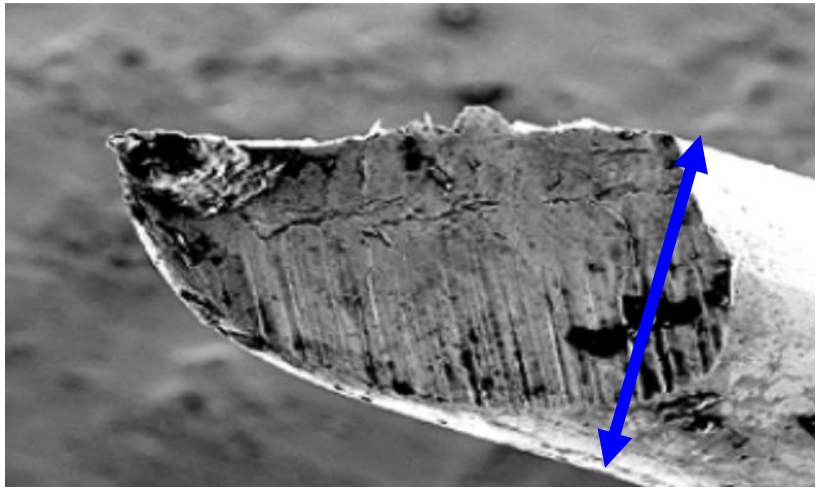

0.2 mm

piezotube

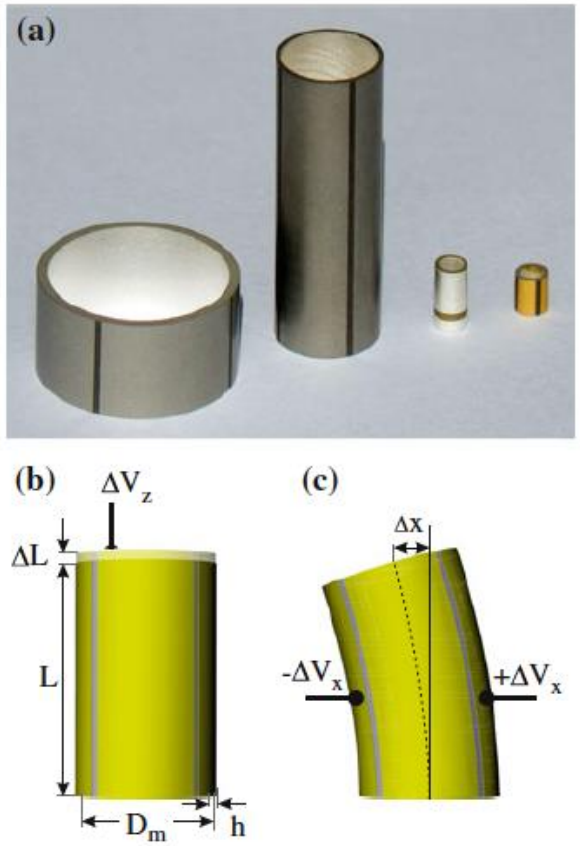

typical parameters (T-dependent):

z: 8 nm/V

x,y: 60 nm/V

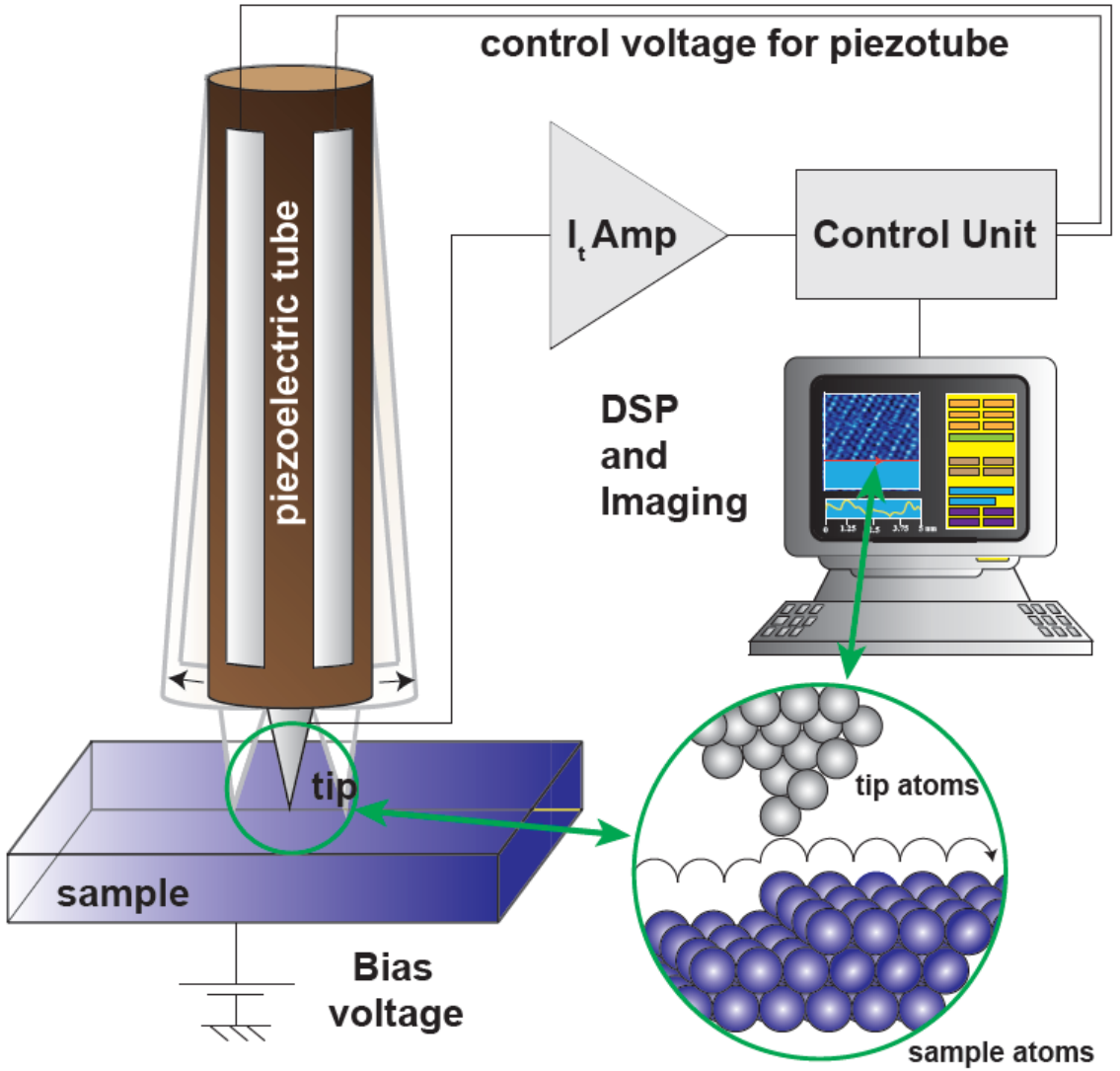

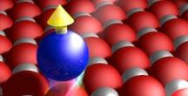

Vibrations and EM noise

Changing the tip-sample distance by 1 Å = 100 pm produces a change of one order of magnitude in the tunneling current

The atomic corrugation (electronic density more localized at the atoms than between the atoms) is of the order 20 pm →
ideally, noise of a few pm max

Sources of vibrations:
building and environment
mechanical pumps
activity in nearby labs

solutions:
design of the STM
vibrational isolation

Sources of electromagnetic noise:
50 Hz from power lines
RF EM waves

solutions:
proper grounding
filters

STM imaging modes

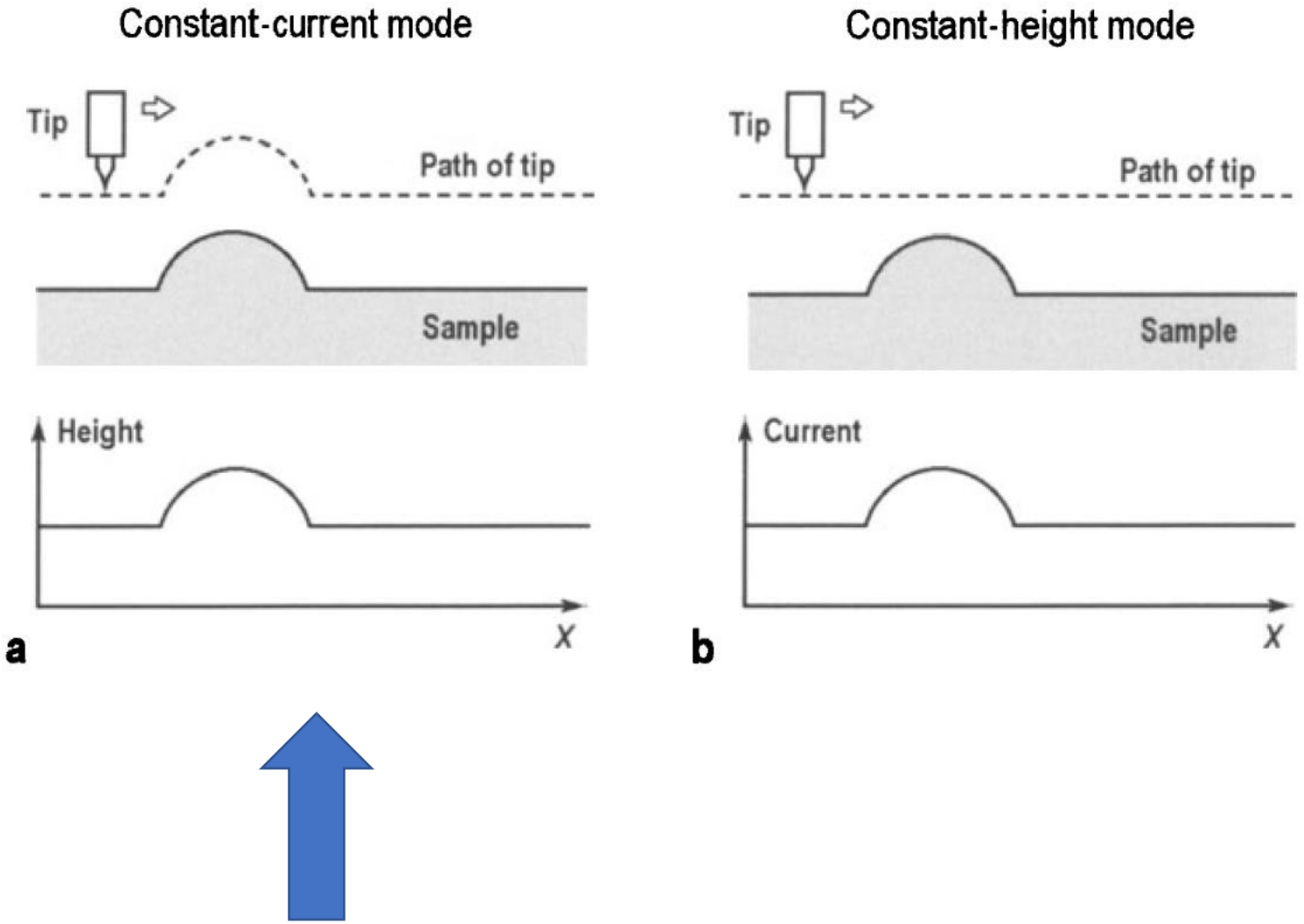

The first published “image”: Si(111)-7x7 reconstructed surface

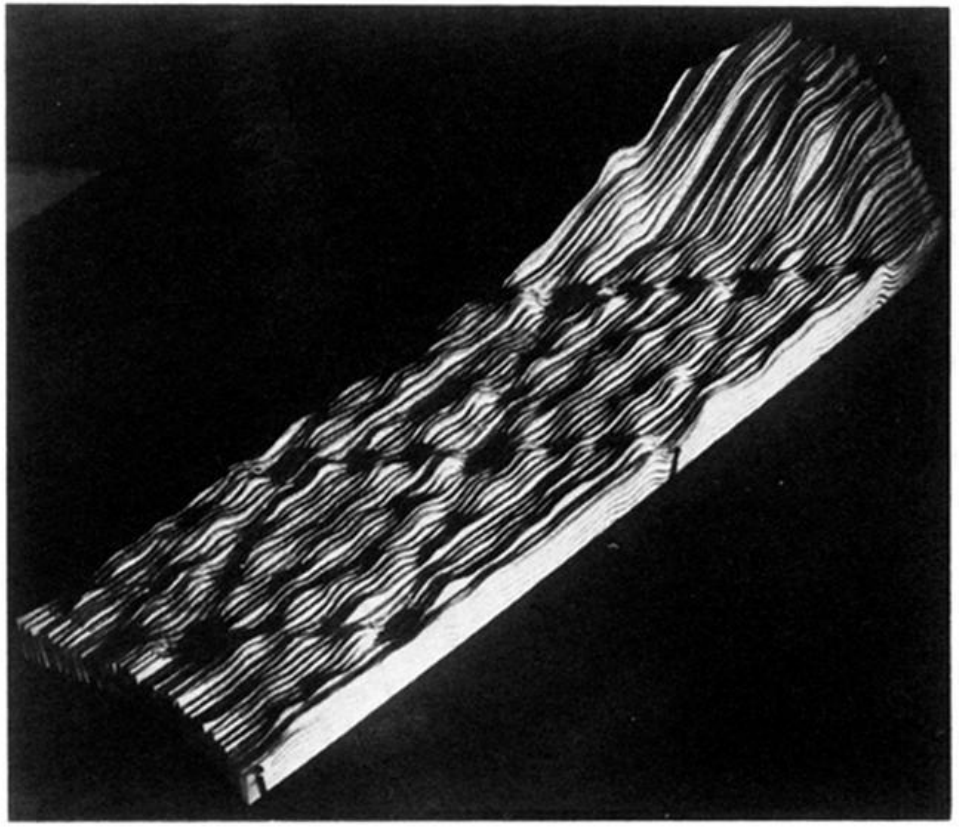

FIG. 1. Relief of two complete 7×7 unit cells, with nine minima and twelve maxima each, taken at 300 °C. Heights are enhanced by 55%; the hill at the right grows to a maximal height of 15 Å. The [$\bar{2}$11] direction points from right to left, along the long diagonal.

today

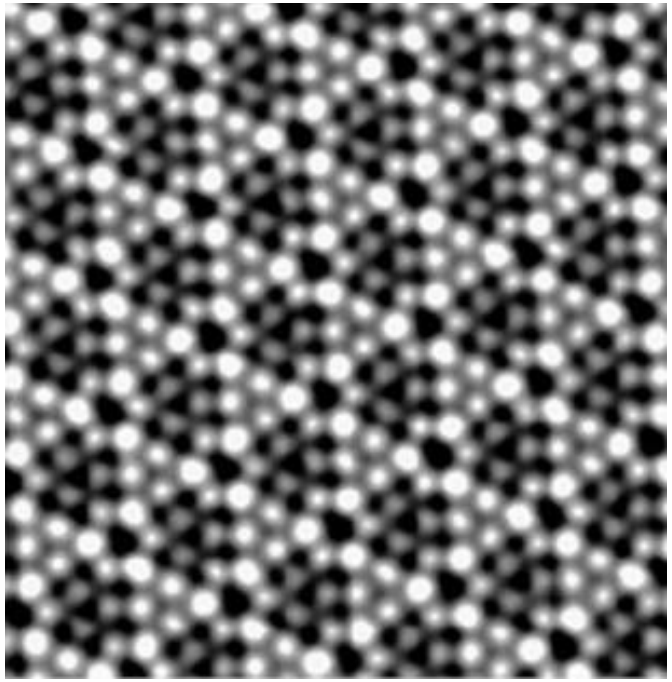

DOI: 10.1103/PhysRevLett.50.120
Phys. Rev. Lett **50**, 120 (1983)

Imaging: Au(111)

Exercises 2.6 – 2.8

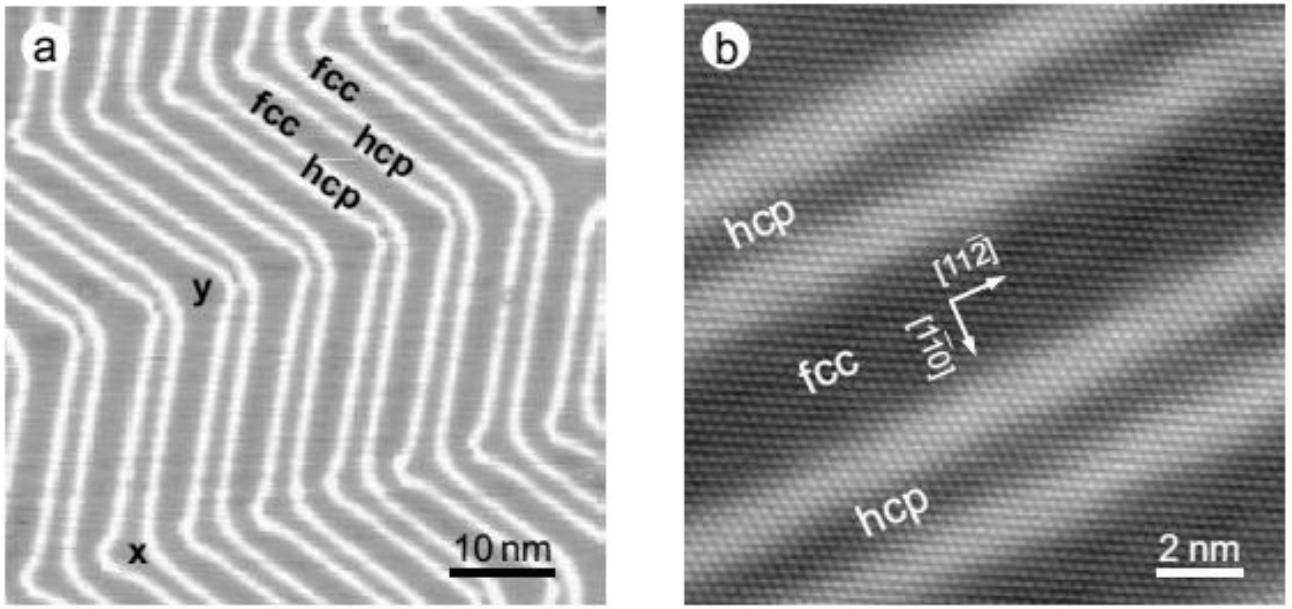

Figure 3.1: STM image showing the herringbone reconstructed Au(111) surface. a) Alternating fcc and hcp stacking domains, as well as *x*- and *y*-type elbows are visible. b) Atomically resolved STM image, revealing the slightly distorted hexagonal arrangement of the surface atoms together with the domain walls separating fcc and hcp stacking. The interatomic distances along $[11\bar{2}]$ and $[1\bar{1}0]$ are 2.88 Å and $\approx$ 2.75 Å, respectively. (Tunneling parameters: a) $V = -0.7$ V, $I = 0.2$ nA; b) $V = -0.02$ V, $I = 1.3$ nA)

M.-C. Blüm,
EPFL PhD thesis

DOI: 0.1103/PhysRevB.42.9307
Phys. Rev. B **42**, 9307 (1990)

Imaging: Ag / Pt(111)

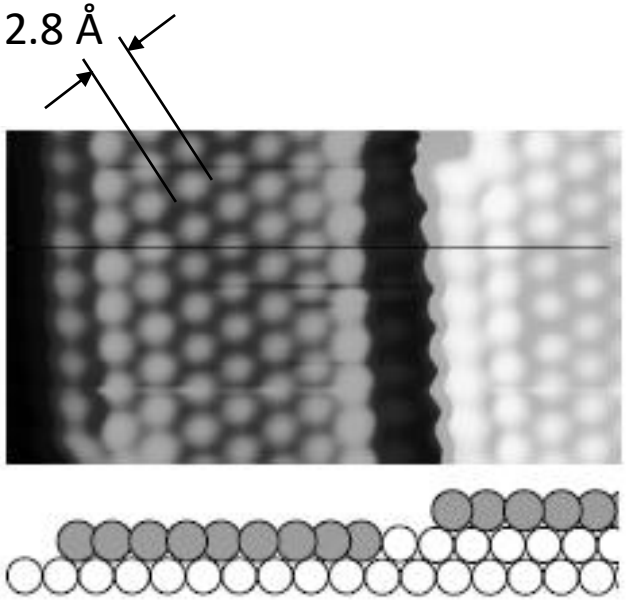

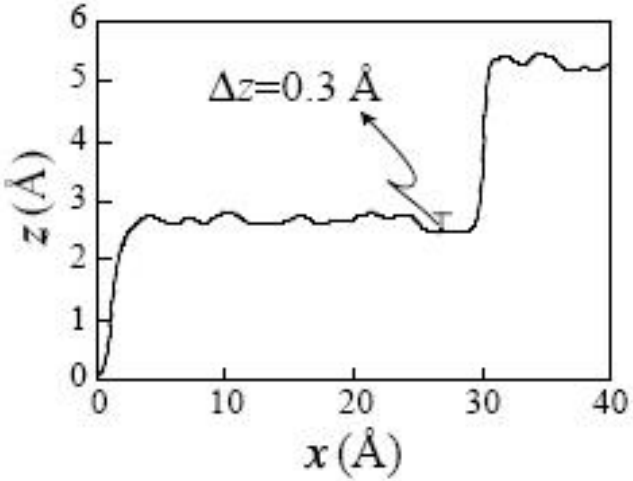

Constant current image of a stepped Pt surface covered by 1 monolayer Ag
(I = 2.7 nA, V = 10 mV)

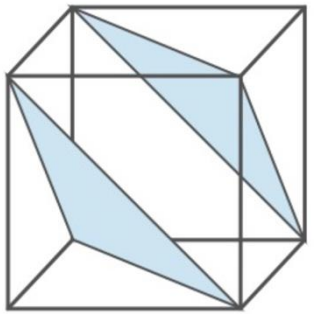

111 planes (Pt fcc, a = 3.9 Å)

P. Gambardella,
EPFL PhD thesis

Imaging: Al(111)

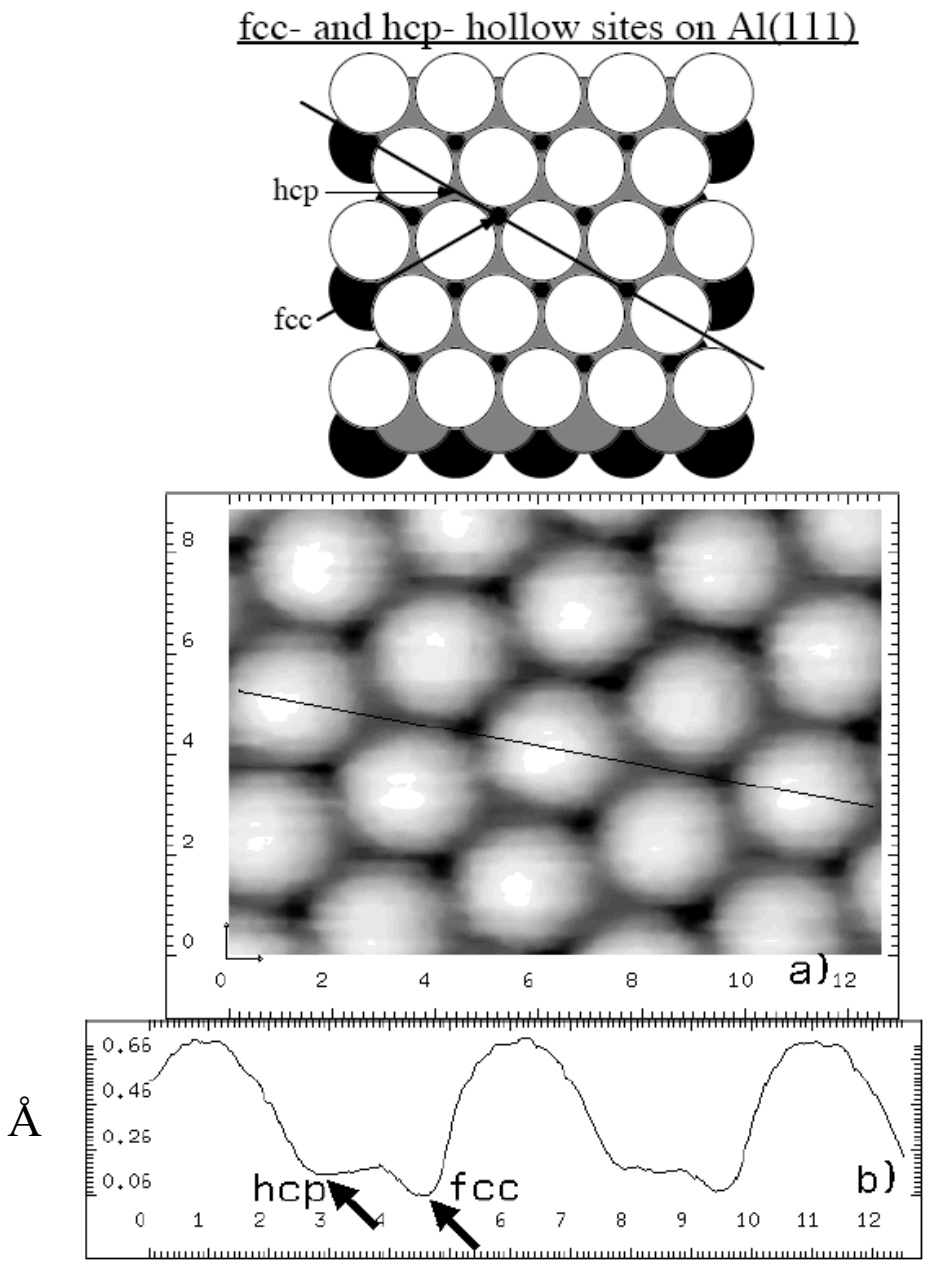

H. Brune, PhD thesis

Imaging: GaAs(110)

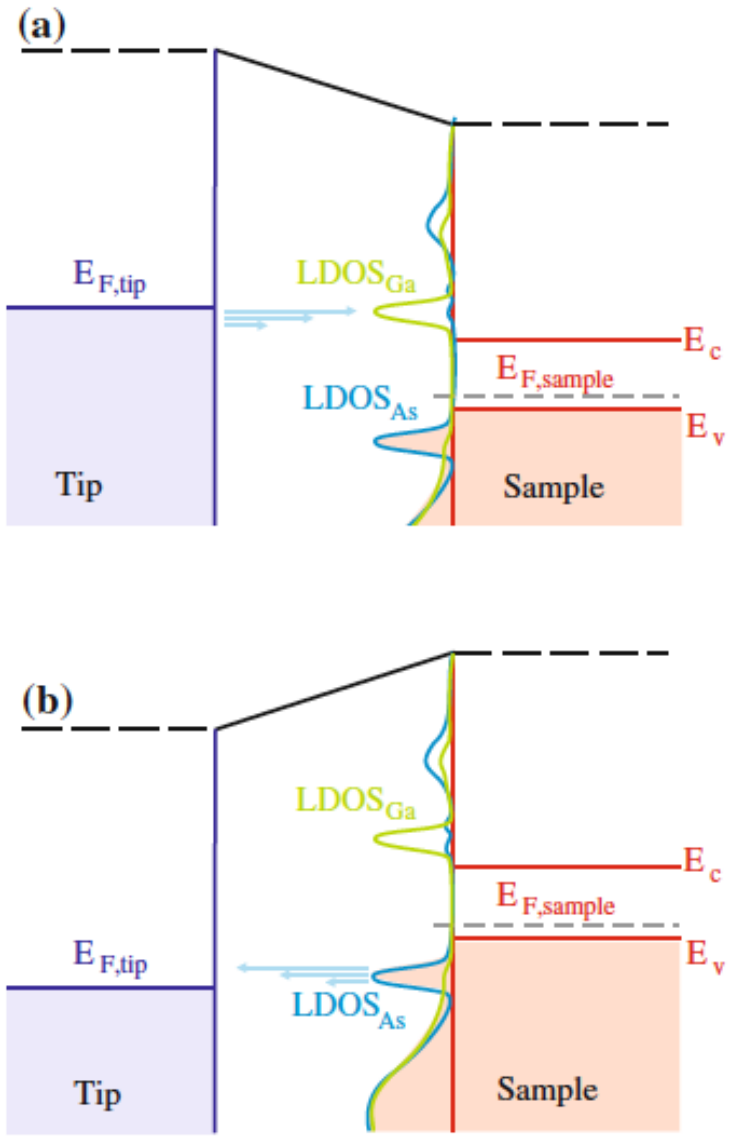

Imaging of non-conductive samples? Only if bias is high enough

Atom-selective imaging of the GaAs(110) surface:
voltage-dependent scanning tunneling microscope images

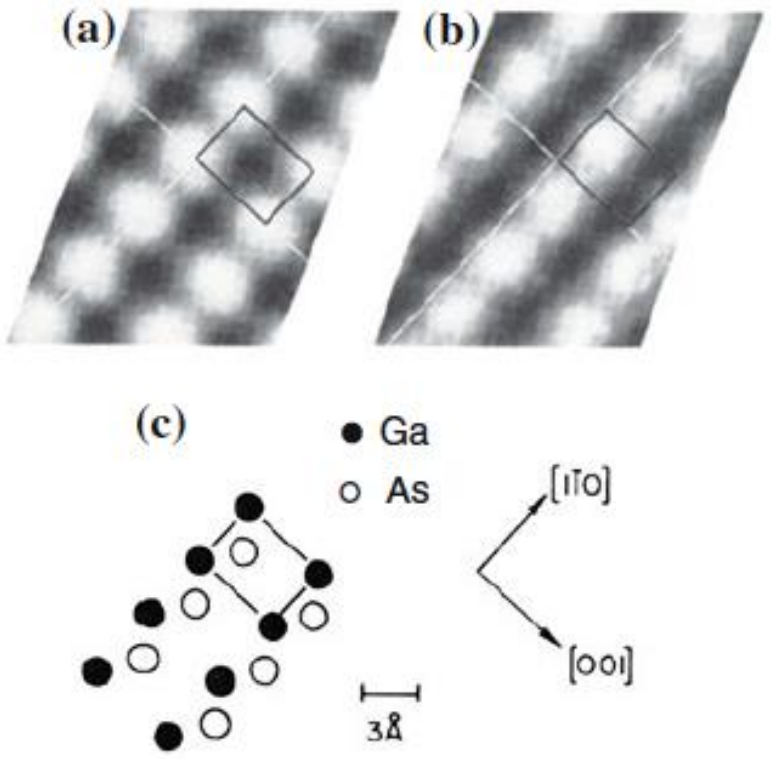

DOI: 10.1103/PhysRevLett.58.1192
R.M. Feenstra et al., Phys. Rev. Lett. **58**, 1192 (1987)

Atomic Force Microscope (AFM)

Exercise 2.9

AFM enables atomic-scale imaging of insulating surfaces

The tip is mounted on a cantilever and is brought very close / into contact with the sample surface.

A force, attractive or repulsive depending on the distance, acts between tip and sample

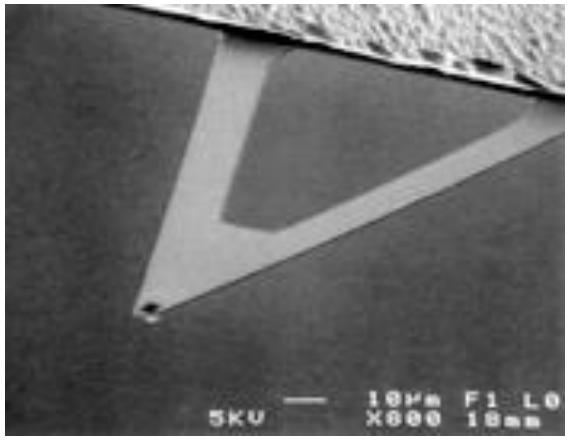

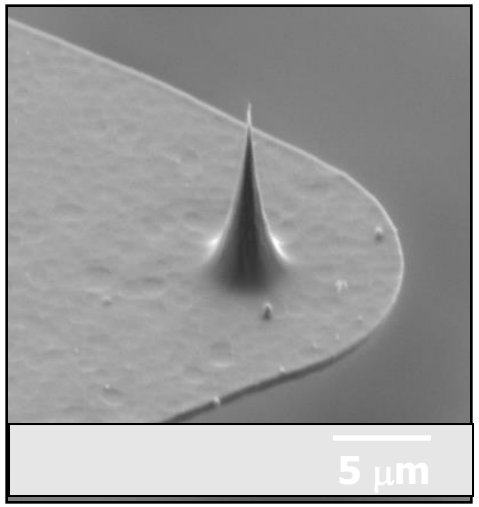

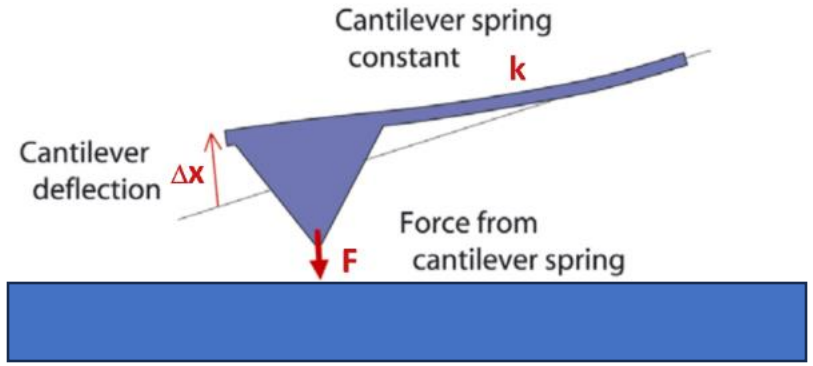

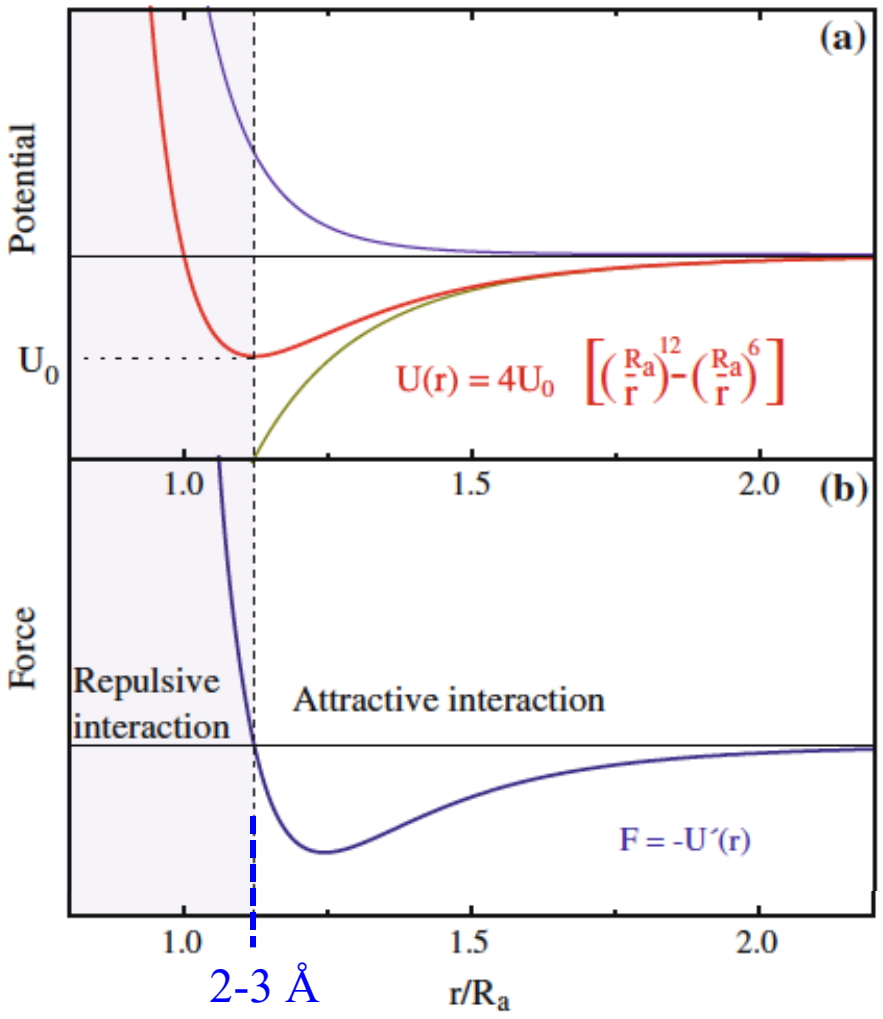

Potential U and force $F = -dU/dr$ between sample and tip vs distance

Lennard-Jones type potential: sum of two terms

repulsive (Pauli), dominates at very short distance

+

attractive (van de Waals), dominates at larger distance

→

minimum

possibly, also chemical bonding at short distance

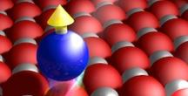

Static force mode

Static mode: typically in contact, in the repulsive regime of force-distance curve

The force on the cantilever is related to its deflection via Hooke's law: $F = -kx$, where k is the spring constant of the cantilever and x is the deflection.

The feedback loop maintains constant the force between the tip and the sample i.e., constant bending of the cantilever.
The corresponding changes in the z-position required to maintain a constant tip-sample distance correspond to the topography of the sample.

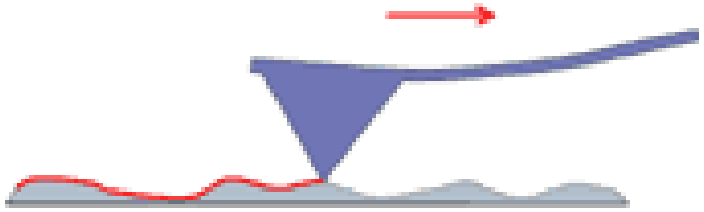

Contact mode: the last atoms of the tip are in direct contact with the surface atoms, not suitable for soft surfaces

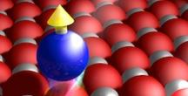

Dynamic force mode

Dynamic modes: typically non-contact, in the attractive regime of force-distance curve

oscillating cantilever:
The cantilever is excited to vibrate close to its free resonance frequency. When tip approaches the surface, the interaction between tip and sample changes the resonance frequency of the cantilever

amplitude modulation (AM) detection scheme:

- fixed drive amplitude and frequency
- change in frequency due to tip-sample interaction results in a shift of the resonance peak, and consequently in a reduced detected amplitude at the drive frequency (off resonance)
- change in amplitude: feedback signal for regulating the tip-sample distance.

frequency modulation (FM) detection scheme:

- cantilever always oscillates at resonance:
- resonance frequency shifts due to a tip-sample interaction, the cantilever oscillation frequency follows this shift
- frequency shift signal: used to control the tip-sample distance via a z-feedback loop

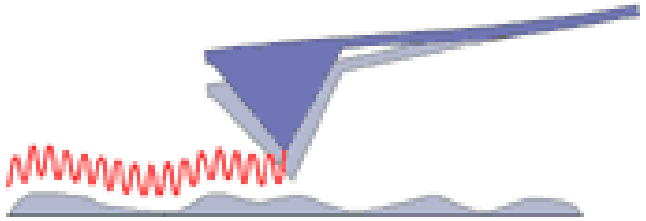

Optical detection of the cantilever deflection

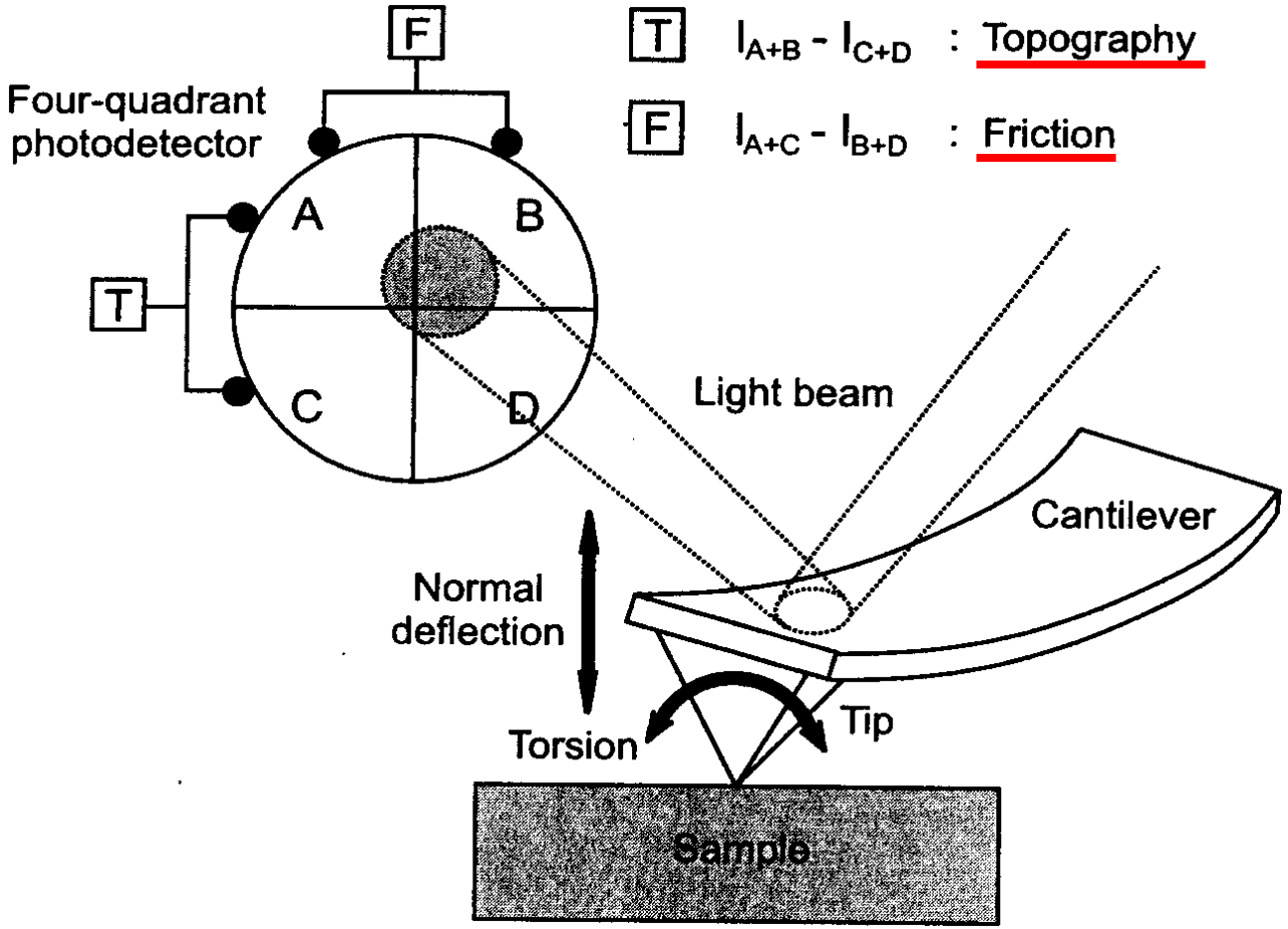

The attractive or repulsive force between the tip and the sample causes a deflection of the cantilever towards or away from the sample.

The deflection is measured by a laser beam directed at the back of the cantilever. As the cantilever deflects, the angle of the reflected beam changes, and the spot falls on a different part of the photodetector.

For non-contact measurements, more sophisticated signal treatment is required.

Contact *vs* non-contact mode

Polymer (soft sample) on a surface

contact

non-contact

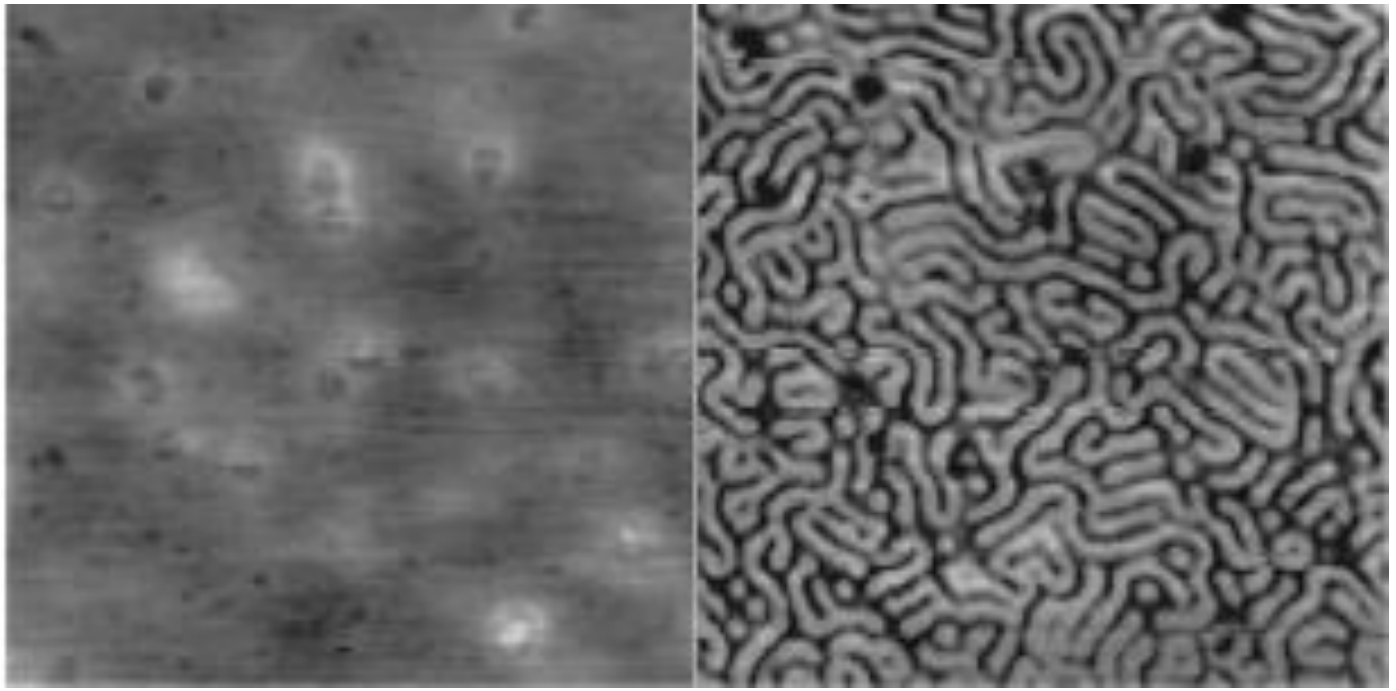

Quartz sensor AFM

Using quartz sensors (for example tuning forks) as oscillators instead of cantilevers:

- the detection of the oscillation signal can be performed completely electrically, without any optical element
- the tip-sample interaction force is transduced to electric signals through the piezoelectric effect of quartz
- with appropriate wiring, it can be used for both AFM and STM

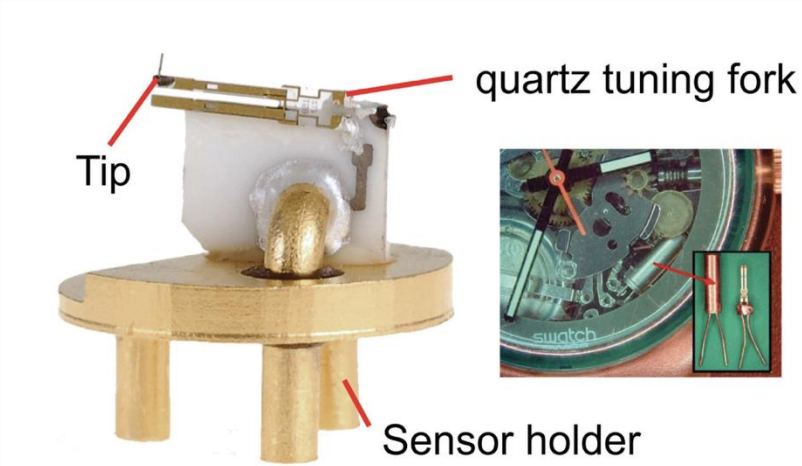

DOI: 10.1063/1.5052264
F. Giessibl, Rev. Sci. Instr. **90**, 011101 (2019)

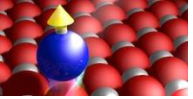

The Chemical Structure of a Molecule Resolved by AFM

CO-functionalized tip

Pentacene / Cu(111)

STM image

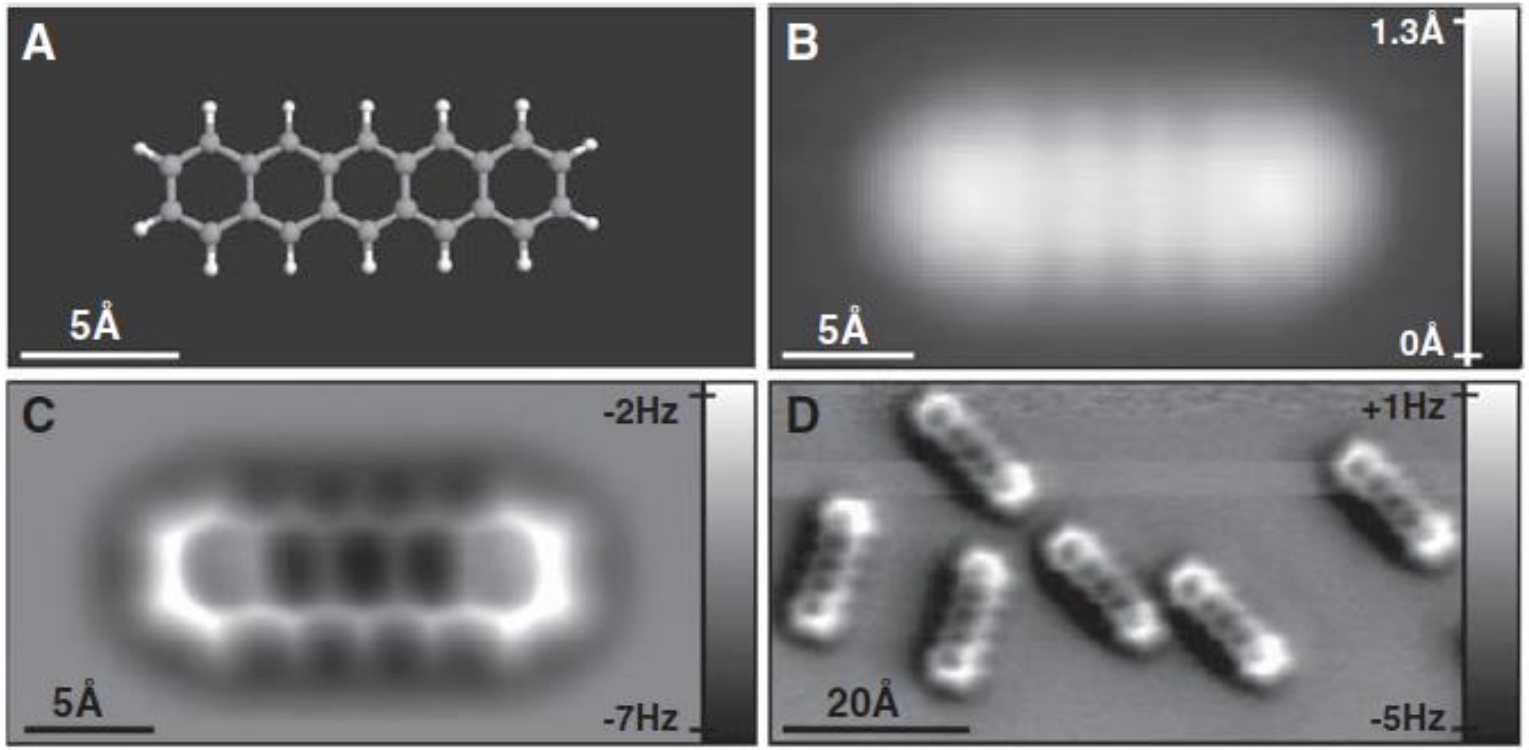

AFM image

DOI: 10.1126/science.1176210
Gross et al., Science **325**, 1110 (2009)